The Transient Characteristics of Arc Channel in Air under Impulse Voltage

By

Hiromu ISA,* and Muneaki HAYASHI*

(Received September 28, 1976)

Abstract

When a breakdown of an air gap occurs under an impulse voltage, a transient arc is observed. In this paper, the transient arc is observed by means of a chopped wave voltage, a micro-photometer etc.. Then, the arc voltage, the arc current density, the arc channel brightness and the channel construction are investigated. As for the results, the resistance, the expanding velocity, the temperature etc. of the arc channel for time were obtained.

1. Introduction

The bridgeover of an air gap by a secondary streamer or a leader due to an impulse voltage causes the main stroke. This corresponds to the last stage in the electrical breakdown process, and its nature is the transient arc.[1,2] So far, most of the studies on the transient arc are concerned with the contacting points of current breakers etc.[3]. A few research results of the arc itself, however, can be found regarding an impulse breakdown.[4] In this study, applying an impulse voltage across a rod-to-plane gap, the arc voltage, the arc resistance, and other physical transient characteristics after the occurrence of a flashover are investigated. Also, the growth of the arc channel and its mechanism are studied.

2. Experimental Apparatus and Measuring Methods

The schematic diagram of the experimental set up is shown in Fig. 1. The condenser (0.05μF), the resistor (330Ω) and the switch S are the main parts of the impulse voltage generator. The current through, and the voltage across, the gap were observed by monitoring the voltage across the resistor R_i and the output voltage

* Department of Electrical Engineering

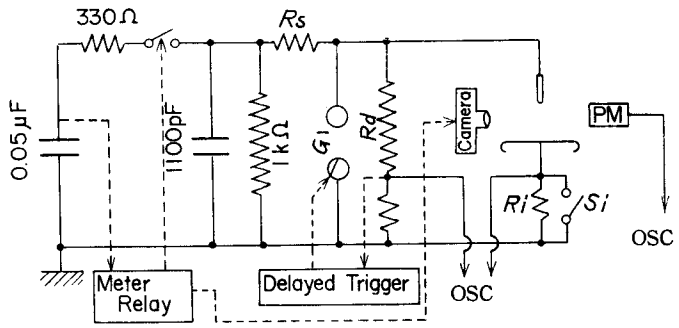

R_d =10kΩ or 80kΩ, R_s =250Ω~40kΩ,
R_i =5~75Ω
G_1 : Gap for Voltage chopping

Fig. 1. Schematic diagram of experimental apparatus.

of R_d with an oscilloscope. R_s is the series resistor limiting the current, and has a value of 250Ω~40kΩ. R_i can be chosen between the range 5~75Ω according to the value of R_s. If necessary, both ends of R_i can be short circuited. The value of R_d was 10kΩ mostly, and only when R_s was 40kΩ, it was 80kΩ. G_1 was used for chopping off the applied voltage and is operated by a delayed trigger circuit which is controlled by the rising up of the applied voltage. The test gap consists of a brass hemispherical rod and a plane. Only a rod having the radius of curvature ρ=2mm was used. The plane electrode is a disc 25cm in diameter and the end is rounded-off with a radius of 1.5cm. The phenomenon occurring in the gap was photographed and at the same time, a photomultiplier set was used to measure the light pulse.

3. Transient Characteristics of the Arc

3.1 Arc Voltage, Arc Current and Arc Resistance vs. Time

When an impulse voltage is applied across a gap, after the bridging over the gap by a leader, an arc takes place and a flashover (abbreviated as FO in the following) state is achieved. The current i_a, the voltage v_a and the light L_t for the whole gap before and after the FO are shown in Fig. 2, where L_t was obtained by removing the slit there by receiving the whole light of the photomultiplier sight. As shown in Fig. 2, there is a sharp increase of L_t pulse and this is most suitable for determining the beginning moment of the arc. Using this method, the data of i_a, v_a, and L_t was measured under 2 sweeping speeds of the oscilloscope after the FO are shown in Fig. 3. v_a was measured by short-ciecuiting R_i. Fig. 4 shows the shapes of i_a and v_a over a wide time range (0.02~100μs). In this figure, after the

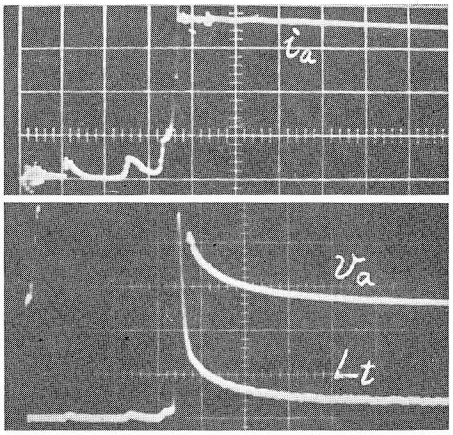

Fig. 2. Variation of i_a, v_a, L_t before and after the flashover. $\rho=2$mm, $\delta=5$cm, rod positive, $V_p=57.7$kV, $R_s=5$kΩ. current: 4.94A/div., voltage: 1.6kV/div., sweep: 0.5 μs/div.

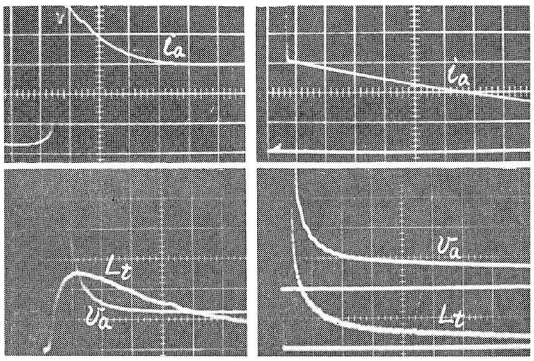

(a) (b)

(a) sweep: 0.1μs/div., current: 74.1A/div., voltage: 8kV/div.
(b) sweep: 2μs/div., current: 74.1A/div., voltage: 400V/div.

Fig. 3 i_a, v_a, L_t vs. time(t). $\rho=2$mm, $\delta=7.5$cm, rod positive, $V_p=89.7$kV, $R_s=250$ Ω.

FO, i_a remains almost unchanged during first 10μs, while v_a decreases rapidly. Further, even if i_a changes 10 times, v_a does not vary so much and the curve line remains almost the same. The variation of the arc resistance $R_a=v_a/i_a$ with time is shown in Fig. 5. R_a decreases rapidly together with v_a, but since v_a does not depend much on i_a, R_a can be considered as inversely proportional to i_a. Further, in order to check the effect of the cathode material on i_a and v_a iron, brass and alminium cathodes were employed. However, for the range $R_s<40$kΩ, no visible difference could be detected.

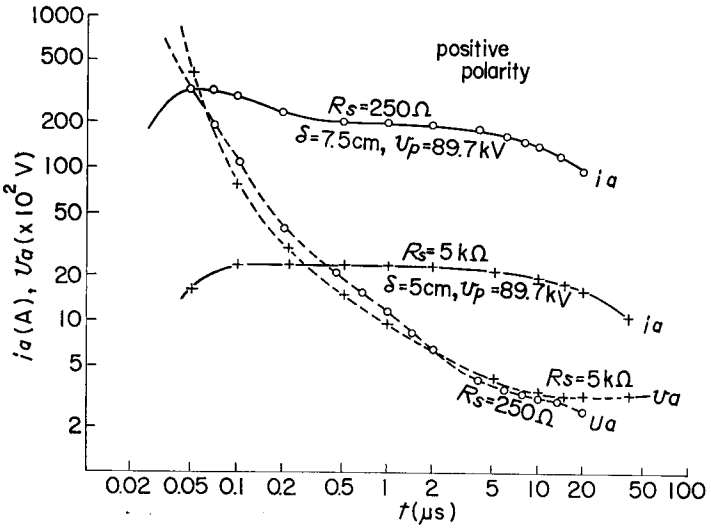

Fig. 4. Example of i_a, v_a vs. t. solid curve: i_a, broken curve: v_a.

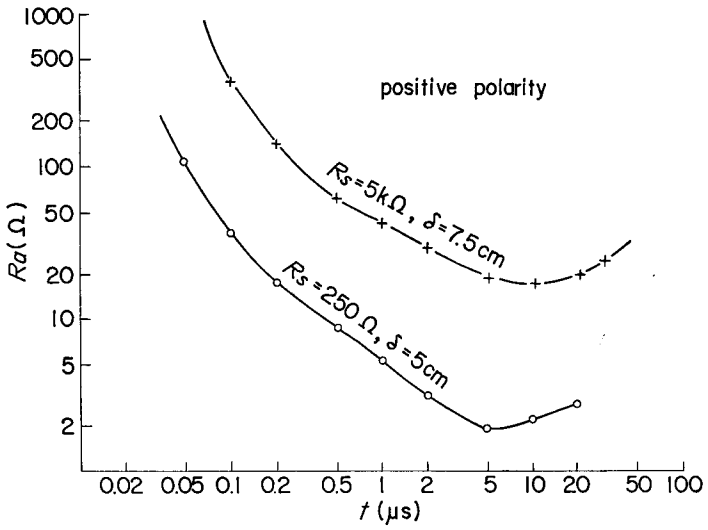

Fig. 5. Characteristics of arc resistance R_a vs. t deduced from the result of Fig. 4.

The product of i_a and v_a at each time shown in Fig. 4 provides the energy consumption data P_a. The variation of P_a and L_t with time is shown in Fig. 6, where L_t can be of any scale. It is deduced that P_a and L_t decrease rapidly with time. The relationship between L_t and P_a can be re-expressed as in Fig. 7. From this figure (excluding the data at just the beginning of the arc formation ($t<0.2\mu$s)),

the relation of $L_t \propto P_a$ can be established approximately.

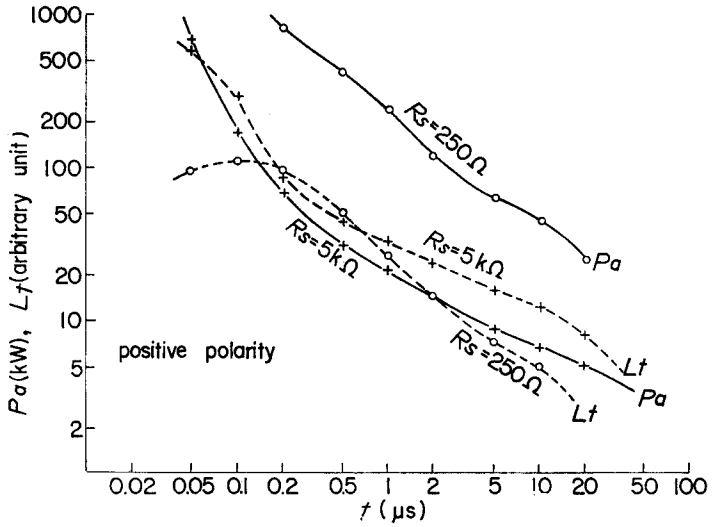

Fig. 6. Characteristics of arc power P_a vs. t and L_t vs. t deduced from the result of Fig. 4.

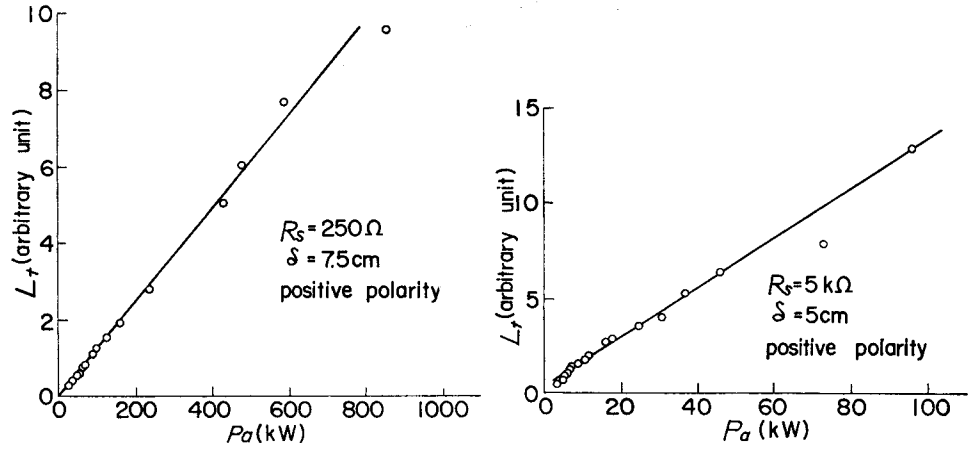

(a) $R_s = 250\Omega$, $\delta = 7.5$cm. (b) $R_s = 5\text{k}\Omega$, $\delta = 5$cm.

Fig. 7. $L_t - P_a$ characteristics (rod positive).

3.2 Arc Characteristic at the Moment of the Minimum Arc Potential

As shown in Fig. 5, the arc resistance R_a at 5~10μs just after the FO is the lowest. Here, as a standard for defining the arc characteristic, the physical values at $t = 5\mu$s are used and are denoted by a suffix 0 (R_{ao}, v_{ao} etc.). Fig. 8 shows the gap length δ vs. v_{ao} with i_{ao} as the parameter. It is deduced that v_{ao} is proportional

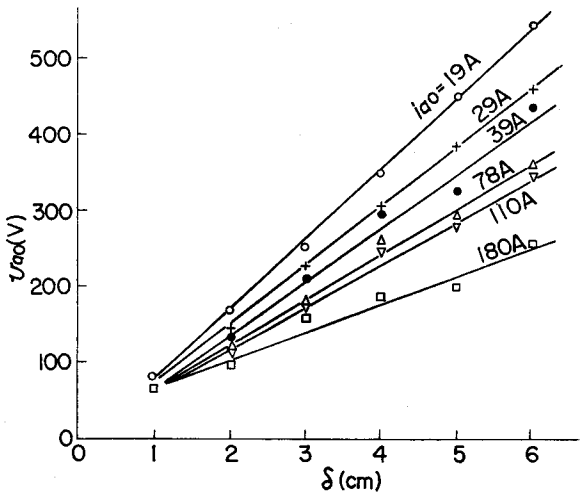

Fig. 8. $\delta - v_{ao}$ characteristics with i_{ao} as a parameter (at $t=5\mu$s).

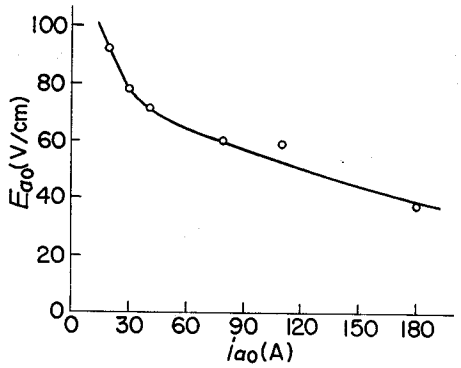

Fig. 9. $E_{ao} - i_{ao}$ characteristics (at $t=5\mu$s).

to δ. And, by extrapolation, when δ tends to 0, $v_{ao} \approx 10$V was obtained. This is a reasonable value of the cathode fall due to the arc. The inclination of the curve in Fig. 8 shows the potential gradient E_{ao} along the arc channel. Fig. 9 shows E_{ao} vs. i_{ao}. In any case, the voltage gradient is about 4~5 times that of a normal arc.[3] Fig. 10 shows R_{ao} vs. δ with i_{ao} as the parameter. And similarly to v_{ao}, $R_{ao} \propto \delta$ is possibly deduced, and its inclination is almost inversely proportional to i_{ao}. The straight lines in Fig. 8 and 10 indicate the uniformity of the voltage gradient along the longitudinal direction of the arc channel.

Fig. 11 shows i_{ao} vs. v_{ao} with δ as the parameter. From this figure, it is dethe duced that for small δ, v_{ao} does not depend on i_{ao} and remains almost constant, and the larger δ becomes, the stronger the influence of i_{ao} becomes. However, for i_{ao} to vary 10 times, v_{ao} varies only 2 times. Fig. 12 shows the relationship between i_{ao} and

R_{ao}, which can be considered approximately as the hyperbolic curve.

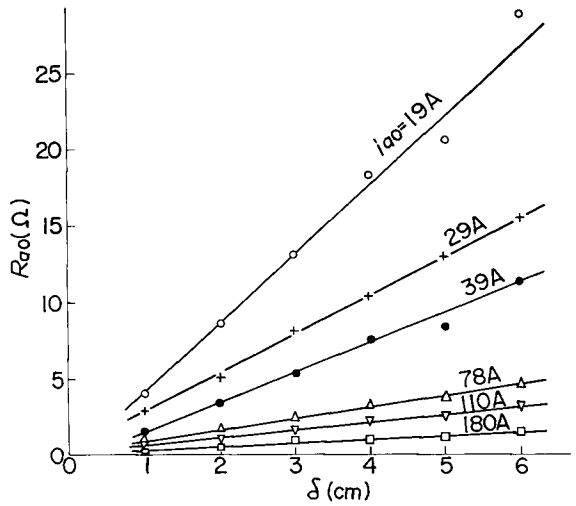

Fig. 10. Characteristics of R_{ao} vs. δ with i_{ao} as a parameter (at $t=5\mu s$).

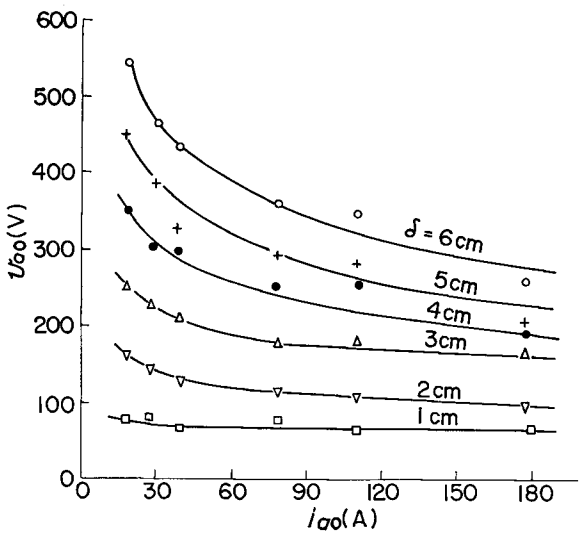

Fig. 11. $i_{ao}-v_{ao}$ characteristics with δ as a parameter (at $t=5\mu s$).

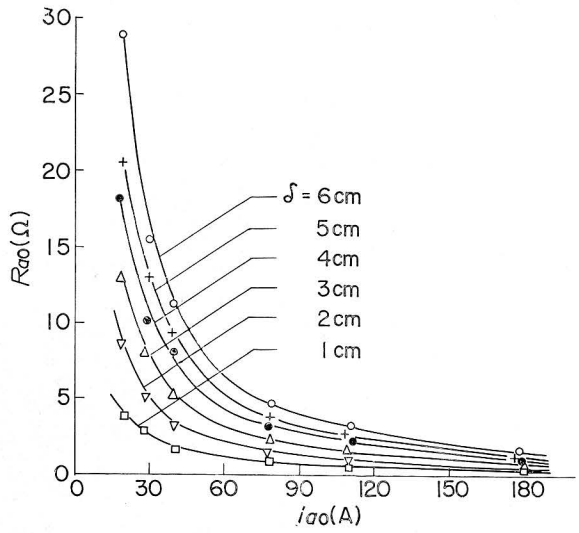

Fig. 12. $i_{ao}-R_{ao}$ characteristics with δ as a parameter (at $t=5\mu s$).

4. Structure and Growth of the Arc Channel

4.1 Structure of the Arc Channel Observed by Still Photograph

〈4.1.1〉 Positive Polarity

The photograph of the FO state obtained by applying a positive impulse voltage to a gap ($\rho=2$mm, $\delta=5$cm and $R_s=250\Omega$) was taken using a light-reducing filter

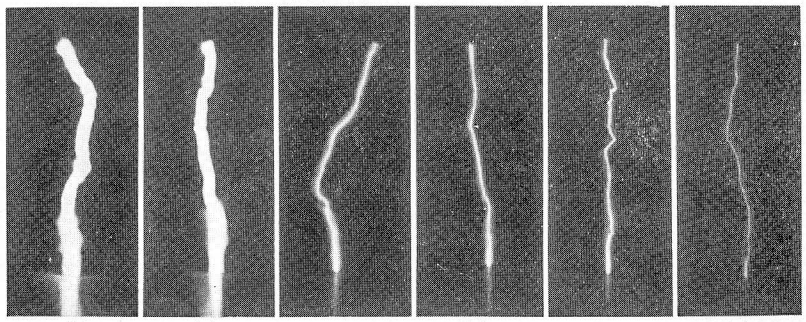

(a) F22, without filter.
(b) F22, with ND4 filter.
(c) F22, with ND16 filter.
(d) F22, with ND32 filter.
(e) F22, with ND64 filter.
(f) F22, with ND128 filter.

Fig. 13. Variation of arc picture for the change of exposure. $\rho=2$mm, $\delta=5$cm, rod positive. $V_p=89.7$kV, $R_s=250\Omega$, lens: f=100mm.

and a lens stop. The ND filter used here is the popular type capable of admitting all visible light. By limiting the exposure, the picture of the arc becomes very thin, and it is necessary to define the arc diameter which is the main problem.

When the exposure is reduced (Fig. 13), the picture of the arc becomes very thin, and at the same time a very thin channel in the central part can be observed (Fig. 13(d), (e)). This part is called the channel core or the 'first region of the arc' in this paper (abbreviated as 'core' in the following). As shown in Fig. 13 (a) and (b), in the bending portion of the arc channel, there is a diffusion of light towards the inner side of the bending. This is probably the diffusion of plasma from the arc channel. (This will be described later.) It consists of the core and the portion, the diameter of which can be varied by different degrees of exposure, which contribute to the conduction of the current. Here, the latter is called the 'second region of the arc'. To summarise the above, the arc channel can be represented by a three-fold structure as shown in Fig. 14(a). The part where the arc comes into contact with the cathode has a structure as shown in Fig. 14(b). Most probably, this is due to an occurrence of the transient glow, which is, however, not confirmed in the current or voltage wave form during the FO.

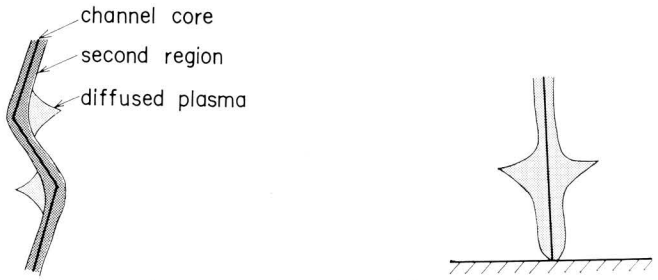

(a) middle part of arc channel. (b) near the cathode region.

Fig. 14. Structure of arc channel.

〈4.1.2〉 Negative polarity

Fig. 15 shows the arc photographs when a negative impulse was applied. In this

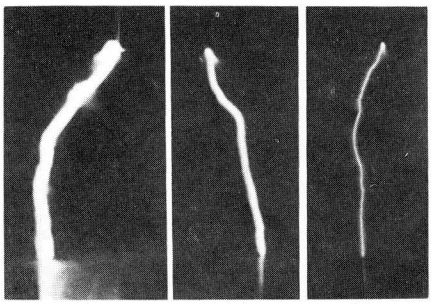

(a) (b) (c)

(a) F8, with ND8 filter.
(b) F16, with ND64 filter.
(c) F16, with ND256 filter.

Fig. 15 Arc picture for negative polarity. $\rho=2$mm, $\delta=5$cm, $V_p=96.6$kV, $R_s=250\Omega$, lens : f= 50mm.

case, there are also channels which have a three-fold structure. Because there is no polarity effect on the arc channel, in the following sections, only those of positive cases are described.

4.2 Measurement of the Brightness Distribution

〈4.2.1〉 Measurement

To investigate the apparent distribution of brightness in the perpendicular direction to the arc channel axis, and in order to eliminate the halation and saturation, an arc photograph taken with a suitable exposure was analysed using a micro-photometer (Narumi NLM-VII type). In this measurement, assuming that the transmissivity of the testing material (photographic film) is T, then the density D of this can be defined as follows:

$$D=\log_{10}(1/T) \tag{1}$$

The range of this measuring instrument was between the maximum value D_{max} and minimum value D_{min}, where $D_{max}-D_{min}=2.5$. In measuring, considering the resolving power $5\mu\times5\mu$ on the testing surface, the area which has a 50μ side length in the axial direction and 5μ in the perpendicular direction to the axis, was adopted as the element of the measuring area, and the sweeping was carried out in the latter direction. Since the exposure E and D of the film has a certain relationship, by using a suitable exposure, it was confirmed that the relationship between D and $\log_{10}E$ can be approximately represented by a straight line with a gradient equal to 1. From this line and the measured value of the density on the film (using JIS standard to develop the Tri-X film), the brightness distribution of the arc channel can be obtained.

〈4.2.2〉 Example of Measurement

Fig. 16 shows the arc photographs and the result of the density measurement.

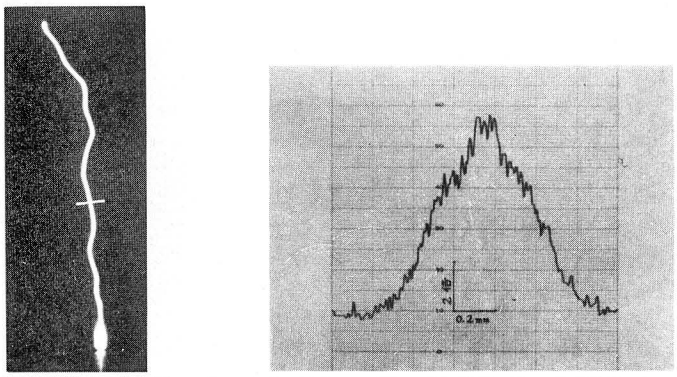

(a) F22, with ND4 filter, lens: f=100mm, V_p=70.7kV, R_s=3.33kΩ, i_{ao}=29A.

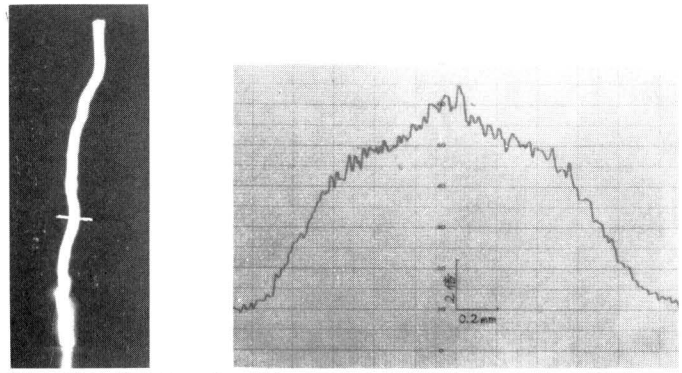

(b) F22, with ND4 filter, lens : f=100mm, V_p=67.4kV, R_s=500Ω, i_{ao}=110A.

Fig. 16. Arc picture and its density distribution perpendicular to the arc channel axis as indicated by a short white line in the figure. ρ=2mm, δ=5cm, rod positive.

Based on this figure, with the density at the center as the standard, and by plotting the normalized value on a straight linescale, the apparent brightness distribution could be expressed as in Fig. 17. From these two figures, it was found that there exists a section in the central part where the brightness is high. This section corresponds to the core in Fig. 14(a). Although it is very easy to distinguish it by the nakedeye, from the result obtained by photometer, the intensity at the center is about twice that of the surrounding area.

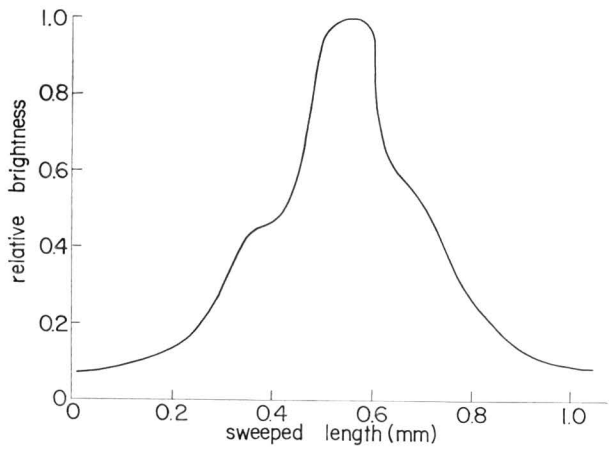

(a) i_{ao}=29A

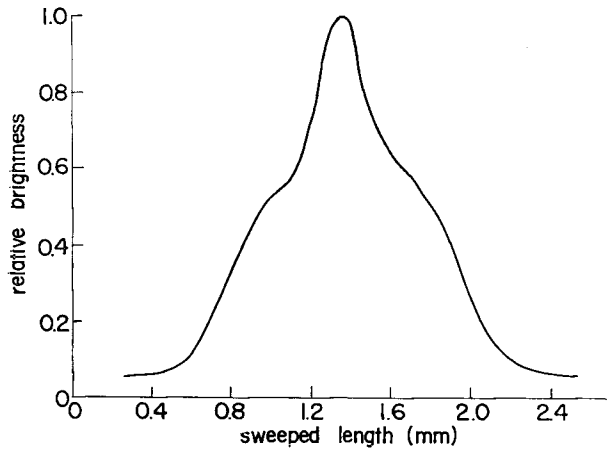

(b) $i_{ao}=110$A

Fig. 17. Brightness distribution of arc channel (reduced in linear scale from the photometer record shown in Fig. 16).

〈4.2.3〉 The Radius and Current Density of the Arc Channel

As described above, the brightness of the arc expands in the direction of its radius. In Fig. 17, if the half-width[5] of the density curve is taken as the channel size, the channel size is equal to that of the core, and is very inconvenient. To improve such a situation, it is proposed here that the point where the density gradient dD/dr is the highest be taken as the radius of the channel r_a. Fig. 18 shows the result of plotting r_a against i_{ao} (at $t=5\mu$s as above defined). In this figure, r_a increases almost linearly with i_{ao}. The average current density of the arc obtained from r_a is shown in Fig. 19. As i_{ao} increases, the current density decreases. The

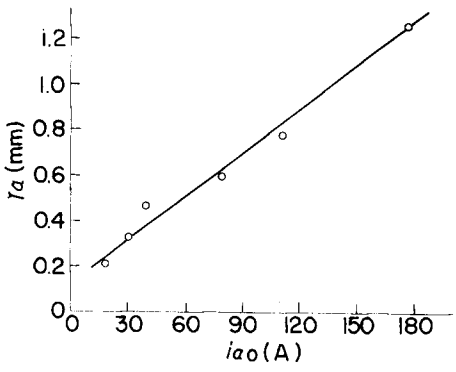

Fig. 18. Radius of arc channel r_a vs. i_{ao}.

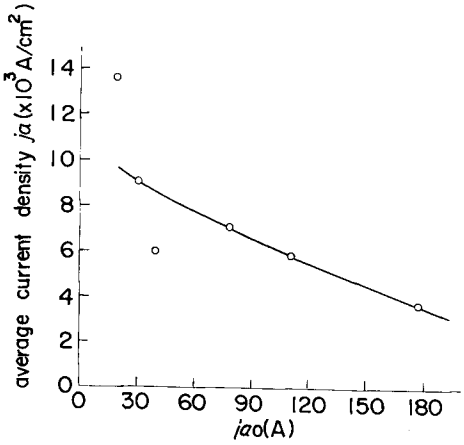

Fig. 19. Average arc current density j_a vs. i_{ao}.

value obtained here is about ten times as much as the values obtained by other researchers (Table 1).[4]

Table 1. Average current density of transient arc.

Flower[4]		Authors	
current (A)	current density (A/cm²)	current (A)	current density (A/cm²)
9	530	18.8	13600
28	800	30.0	9000
55	1040	38.8	6000
84	1000	78	7000
400	1330	110	5800
		177	3600

4.3 The Growth of the Arc Channel

When the applied voltage was chopped off at the various time T_c after the FO, the current wave form i_a, the arc voltage v_a, the brightness of the whole gap L_t and a still photograph were obtained; and the arc channel development following an impulse breakdown was investigated.

〈4.3.1〉 The Change of the Arc Appearance

Fig. 20 shows the experimental results when $R_s=1\text{k}\Omega$. It can be seen in Fig. 20(a) and (b) that the core is formed at a very early stage ($T_c<0.2\mu$s). Furthermore, since it has a few sharp bendings, the core is considered to have developed from the leader channel. When $T_c=1\mu$s, the channel expansion can be observed from the photograph. The developed part is the second region, while the core remains almost unchanged (Fig. 20(d)～(f)). The growth slows down its expansion after reaching a certain level, and even without chopping off the applied voltage, the growth does not develop above this level (Fig. 20(g)). In Fig. 20(g), the core is slightly shifted from the central position, which is considered because of the assymetric growth of the second region.

As described above, in the bending part of the arc, a weak light-emission can be observed. The probable causes of this phenomenon are as follows:

(1) Halation or irradiation

(2) The shock wave due to the channel expansion

(3) Ionization by arc light-emission

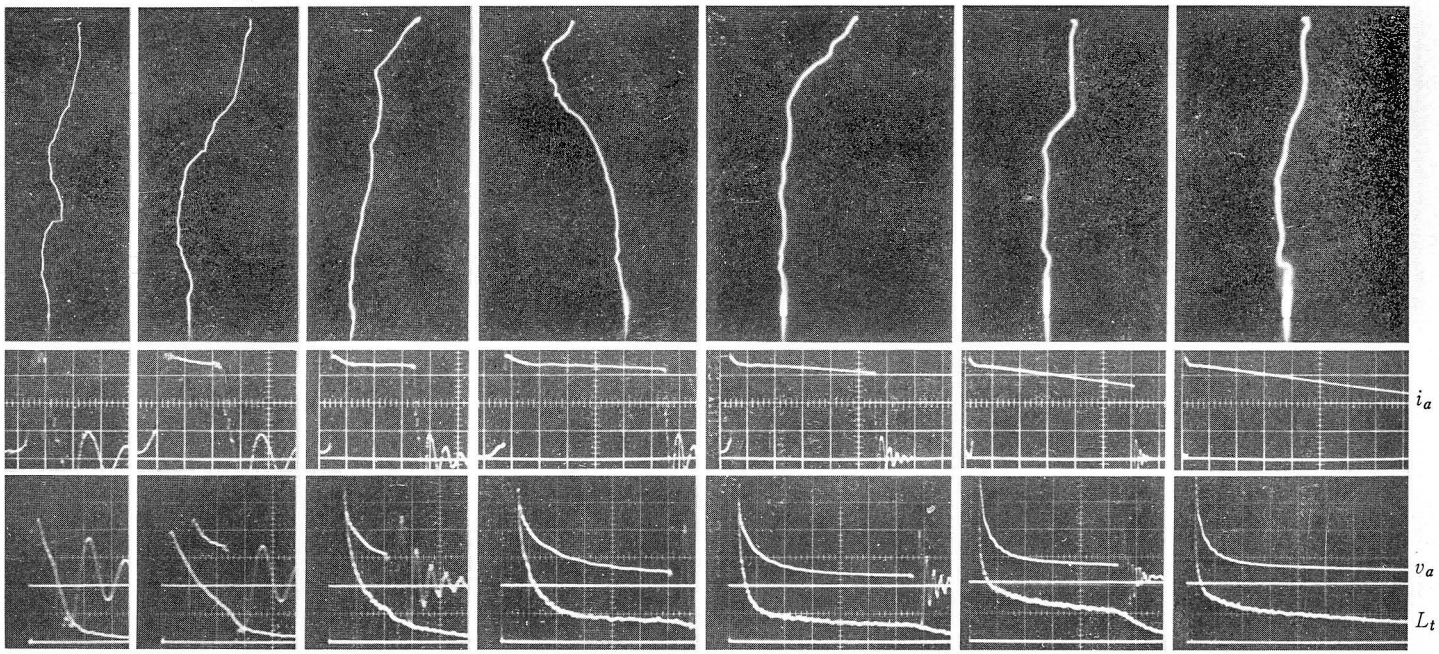

(a) sweep : 0.2μs/div., voltage : 1.6kV/div., $G=1$.
(b) sweep : 0.2μs/div., voltage : 1.6kV/div., $G=1$.
(c) sweep : 0.5μs/div., voltage : 800V/div., $G=2$.
(d) sweep : 0.5μs/div., voltage : 800V/div., $G=2$.
(e) sweep : 1μs/div., voltage : 800V/div., $G=2$.
(f) sweep : 2μs/div., voltage : 400V/div., $G=4$.
(g) sweep : 2μs/div., voltage : 400V/div., $G=4$.

Fig. 20. Growth of arc channel. $\rho=2$mm, $\delta=5$cm, $V_p=71.3$kV, $R_s=1$kΩ, lens : f=100mm, F22, with ND8 filter, G : relative sensitivity of light pulse measurement, current : 22.2A/div.

(4) The plasma diffusion

Concerning (1), in an under-saturation of the film density, the phenomenon can be observed even under a reduction of light from the arc, and hence it cannot be the effect of halation. Further, the spread by irradiation shows a very small stain[6] (smaller than a few μ) in the picture, and thus it could not be the cause. Concerning (2), even when the channel expansion has an under-velocity of sound, the weak light emission can be observed, and hence this is not the cause either. Concerning (3), the phenomenon could not be observed in a time range less than 1μs where the light intensity is highest and thus it could not be the cause. About (4), assuming a 2-dimensional diffusion, the radius of diffusion r_d is

$$r_d = \sqrt{4Dt} \tag{2}$$

where D: diffusion coefficient, t: time

D is the ambipolar diffusion coefficient. Since $D=0.2\text{cm}^2/\text{s}$[3] in air of 760mmHg, 300 K, then $r_d=0.03$mm at $t=10\mu$s. Assuming the temperature of the channel to be 10^4K, r_d has a value of about 0.1mm, and this is the value which could be distinguished. When $T_c=12\mu$s, the light emission can be confirmed as show in Fig. 20(f). From the above reasons, it could be considered that the weak light emission section consists of the plasma diffused from the channel.

〈4.3.2〉 The Variation of Brightness Distribution with Time

Fig. 21 shows an analytical result of the arc picture by means of a microphotometer. From this figure, the following are deduced;

(a): The core formation starts at $T_c=0.2\mu$s. (b): The brightness at the center is doubled, and then the core formation is completed. (c): The channel expansion starts. (d)$\sim$(f): The expansion of the second region of the channel continues for $T_c=3\sim12\mu$s. (g): The weak light emitting section extends to 2mm in diameter if a full wave (without chopping) is applied.

Fig. 22 shows the variation of the brightness at each part, with the distance r from the channel center as a parameter. The core ($r=0$, 0.1mm) is formed within 1μs. The gradient of the curve in this figure gives the brightness of the picture at a point distance at that time, because the curve shows an integrated value of brightness with time. Hence, the following qualitative deduction can be obtained:

(1) For $r=0$, 0.1mm, at $t>1\mu$s, the brightness decreases. (2) For $0<r<0.35$mm, the greater r is, the smaller the maximum brightness becomes. (3) For $t>3\mu$s, the brightness is almost equal for $0<r<0.35$mm. (4) For $r>0.4$mm, the greater r is, the smaller the brightness becomes.

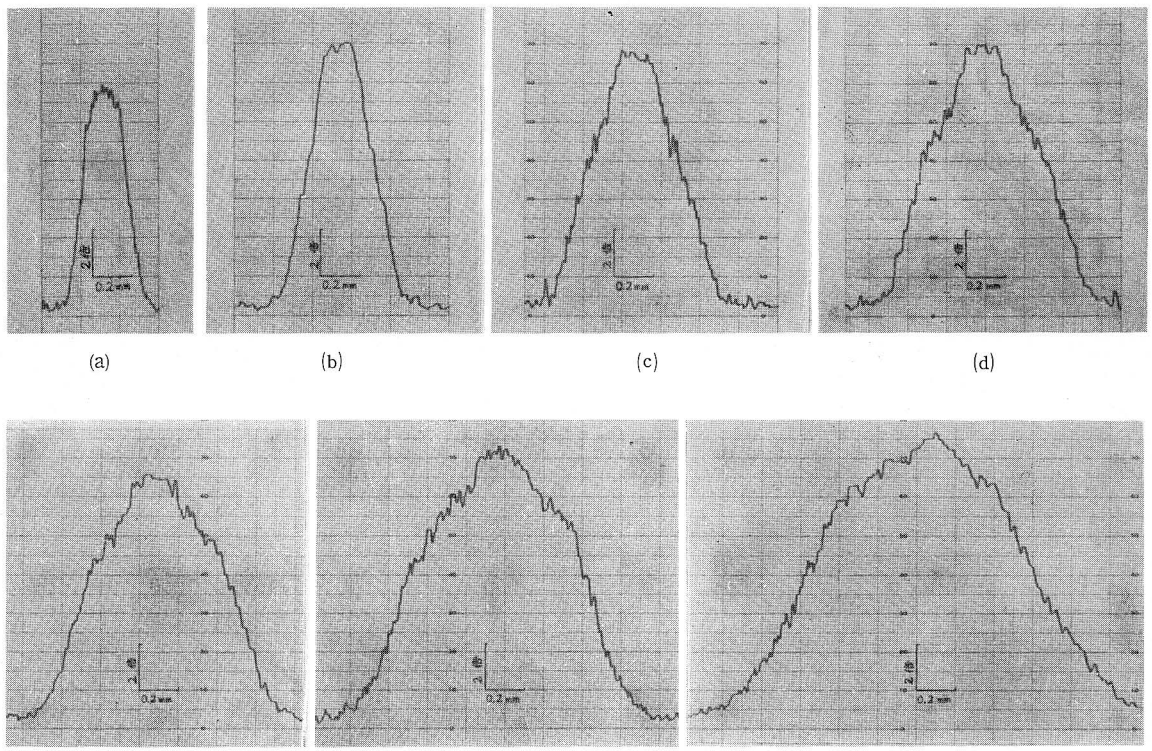

Fig. 21. Density distribution of arc picture shown in Fig. 20 (scanning perpendicularly to the arc channel axis).

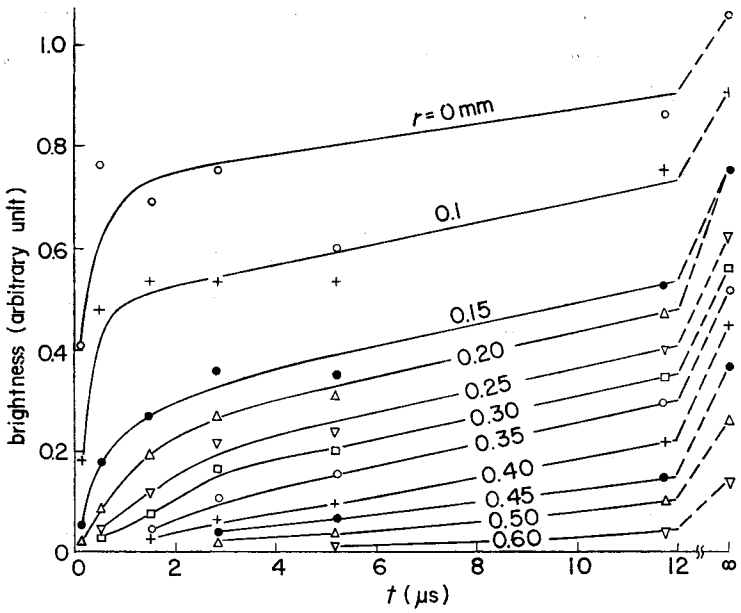

Fig. 22. Variation of each part of arc channel vs. time.

⟨4.3.3⟩ The Expanding Velocity of the Arc Channel

The arc radius r_a has the same definition as given in the previous section, and its expansion with time is as shown in Fig. 23 with i_{ao} as the parameter. The larger

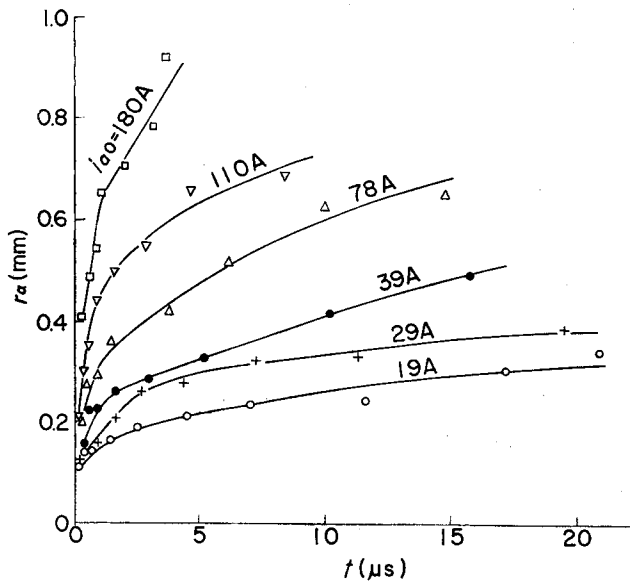

Fig. 23. Characteristics of arc radius r_a vs. t with i_{ao} as a parameter.

the i_{ao} is, the bigger r_a is. The expansion velocity decreases rapidly with time. During the time $t=0\sim1\mu s$, the average volocity becomes subsonic when i_{ao} is below 80A and supersonic if above 80A.

4.4 The Estimation of the Arc Channel Temperature

Assuming that the arc current density j_a after the FO is uniform within the arc channel, the calculated current densities from the experimental results are shown in Fig. 24, with i_{ao} as the parameter. In all cases, the values of j_a coincide with those obtained by other researchers.[4]

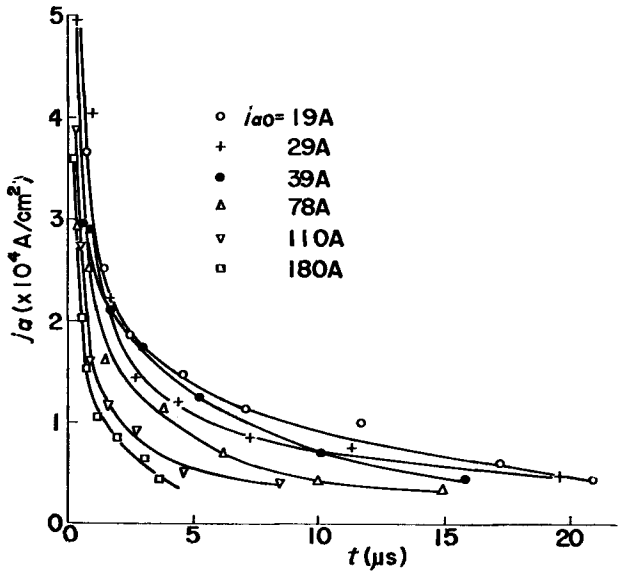

Fig. 24. Characteristics of arc current density j_a vs. t with i_{ao} as a parameter.

Fig. 25 shows the potential gradient of the arc vs. time. In all cases, with $3\mu s$ after the FO, the gradient drops below 100V/cm. Fig. 26 shows the variation of conductivity σ (i_a/E_a) with time. In this figure, the obtained data are scattered widely. Between $1\sim3\mu s$, a peak value of $100\sim200$℧/cm appears, and then decreases. According to Braginskii,[7] the relation between σ and the temperature T of the atmospheric air can be expressed as follows;

$$\sigma=128\sqrt{T} \tag{3}$$

where σ: conductivity (℧/cm), T: temperature (eV)

On the other hand, in the presence of an electric field, the temperatures of the gas and of the electron are different from each other. In atmospheric air,[8]

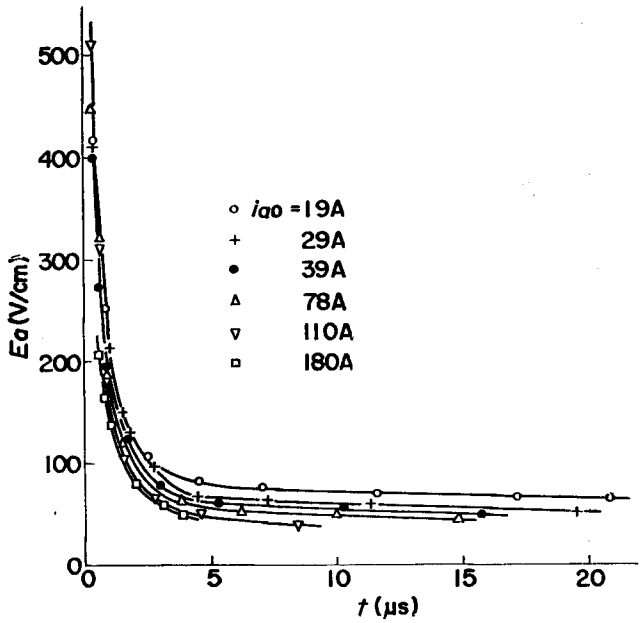

Fig. 25. Characteristics of arc potential gradient E_a vs. t with i_{ao} as a parameter.

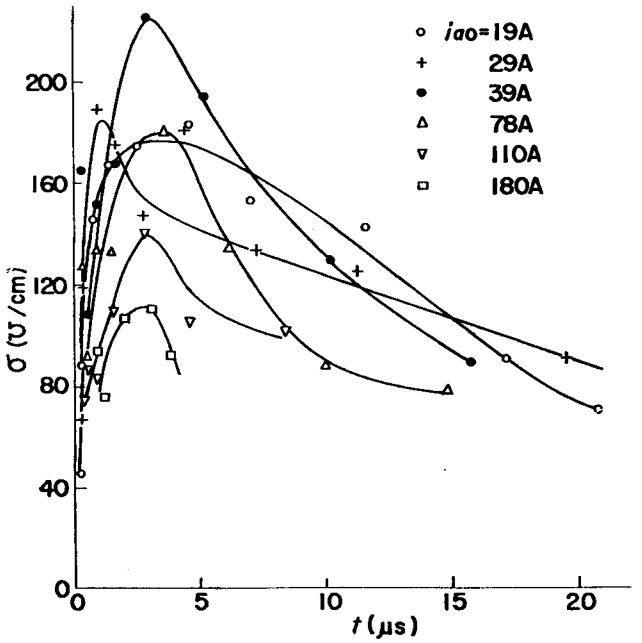

Fig. 26. Characteristics of arc conductivity σ vs. t with i_{ao} as a parameter.

$$T_e/T_g=\sqrt{1+E^2/57.8} \tag{4}$$

where, T_e, T_g: the temperature of the electron and the air respectively, E: field intensity (V/cm)

Fig. 27 shows T_e/T_g vs. time, obtained from Fig. 25 and Eq. 4. T_e/T_g decreases to a value below 2 after 2μs from the FO.

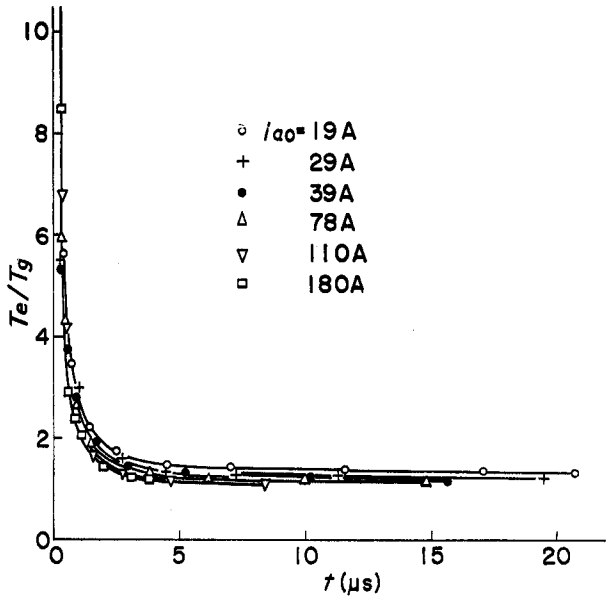

Fig. 27. Characteristics of T_e/T_g within arc channel vs. t with i_{ao} as a parameter.

Eq. 3 is obtained under the assumption of the existence of heat equilibrium. Therefore, it is not applicable to the arc in which T_e is not equal to T_g. However, since the electron mobility is much larger than ion and most of the arc current is transported by electrons, it is possible to substitute T by T_e. From this approximation, being based on σ in Fig. 26, T_e and T_g can be obtained as shown in Fig. 28 and 29. From both figures, T_e and T_g gradually decrease after reaching a maximum value at 2~5μs. The maximum value of T_e and T_g are $6\sim20\times10^3$ K and $5\sim17\times10^3$ K, respectively. For the large i_{ao}, the temperature becomes lower and the reason is not yet known. Most probably, it is due to the limitation of measuring methods. In other words, since the temperature is inversely proportional to r_a^4, the error of measurement increases greatry.

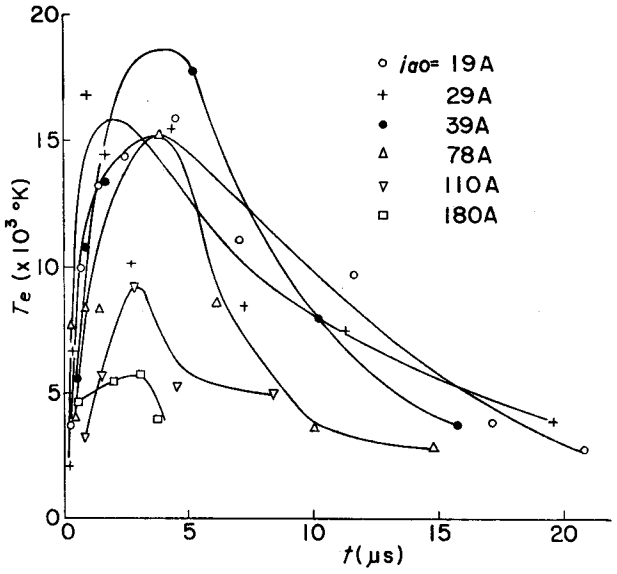

Fig. 28. T_e-t characteristics of arc with i_{ao} as a parameter.

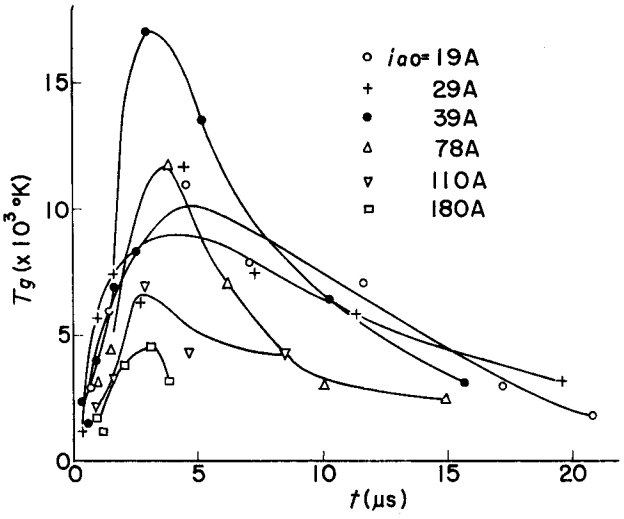

Fig. 29. T_g-t characteritics of arc with i_{ao} as a parameter.

5. Conclusion

In this study, the various characteristics of the arc occurrence and its development after the breakdown of a rod-plane gap were investigated, and the following results were obtained.

(1) After the FO, although the arc current is constant, the arc voltage and the arc

resistance decrease rapidly. For a gap greater than 1cm, the difference in the cathode material does not have any influence on the arc voltage for this phenomenon.

(2) By extrapolation on the curve of the gap length vs. the arc voltage, the voltage drop at the cathode is assumed to be about 10V.

(3) 5μs after the FO, the potential gradient along the transient arc is 40~90V/cm, and is about 4~5 times larger than that of a normal arc.

(4) The voltage-current characteristic of a transient arc has the same tendency as a normal arc and shows a negative characteristic.

(5) An arc channel is made up of three components: the core, the second region and the diffusing plasma.

(6) The shape of the channel core is the same as the leader channel and is formed within 0.1~0.2μs. After about 1μs from its occurrence, it shows the same brightness as the surrounding second region.

(7) Within the arc channel, only the second region develops as time elapses.

(8) The average current density of the transient arc is about $3\times10^3\sim10^4 A/cm^2$.

(9) The larger the current is, the larger the radius of the arc becomes, and its expanding velocity decreases with time.

(10) In the transient arc, the temperatures of both the electron and the gas reach the peak within 1~5μs from its occurrence, and decrease after that. The maximum values are estimated to be $6\sim20\times10^3$ K and $5\sim17\times10^3$ K, respectively.

Lastly, this study was assisted by Prof. Uenosono's helpful advice and by the Scientific Research Fund of The Department of Education of the Japanese Government. The authors would like to express their sincere thanks for all such kind assistance.

References

1) Saxe, J. H., Meek, J. M.: P. I. E. E. **102**-c (1955) 221
2) Hudson, G. G., Loeb, L. B.: Phys. Rev. **123** (1961) 29
3) I. E. E. Japan: Handbook of Discharge Phenomena, OHM-sha (1974)
4) Meek, J. M., Craggs, J. D.: Electrical breakdown of gases (1953)
5) Inaba, T., Kitoh, Y., Miyaji, I.: Trans. I. E. E. Japan **93**-A (1973) 78
6) Miyamoto, G.: Sensitive Materials for Photograph, Kyoritsu-syuppan (1965)
7) Braginskii, S. I.: Soviet Phys.-JETP **34** (1958) 1068
8) Yamamoto, K.: Trans. I. E. E. Japan **3** (1951) 87